The Astrophysical Journal Letters, 750:L2 (6pp), 2012 May 1 doi:10.1088/2041-8205/750/1/L2

STRONG EVOLUTION OF X-RAY ABSORPTION IN THE TYPE IIn SUPERNOVA SN 2010jl

Poonam Chandra[1], Roger A. Chevalier[2], Christopher M. Irwin[2], Nikolai Chugai[3], Claes Fransson[4], and Alicia M. Soderberg[5]
[1] Department of Physics, Royal Military College of Canada, Kingston, ON, K7K 7B4, Canada; Poonam.Chandra@rmc.ca
[2] Department of Astronomy, University of Virginia, P.O. Box 400325, Charlottesville, VA 22904-4325, USA
[3] Institute of Astronomy of Russian Academy of Sciences, Pyatnitskaya St. 48, 109017 Moscow, Russia
[4] Department of Astronomy, Stockholm University, AlbaNova, SE-106 91 Stockholm, Sweden
[5] Smithsonian Astrophysical Observatory, 60 Garden St., MS-20, Cambridge, MA 02138, USA
Received 2012 February 7; accepted 2012 March 23; published 2012 April 4

ABSTRACT

We report two epochs of *Chandra*-ACIS X-ray imaging spectroscopy of the nearby bright Type IIn supernova SN 2010jl, taken around two months and then a year after the explosion. The majority of the X-ray emission in both spectra is characterized by a high temperature ($\gtrsim$10 keV) and is likely to be from the forward shocked region resulting from circumstellar interaction. The absorption column density in the first spectrum is high ($\sim 10^{24}$ cm^{-2}), more than three orders of magnitude higher than the Galactic absorption column, and we attribute it to absorption by circumstellar matter. In the second epoch observation, the column density has decreased by a factor of three, as expected for shock propagation in the circumstellar medium. The unabsorbed 0.2–10 keV luminosity at both epochs is $\sim 7 \times 10^{41}$ erg s^{-1}. The 6.4 keV Fe line clearly present in the first spectrum is not detected in the second spectrum. The strength of the fluorescent line is roughly that expected for the column density of circumstellar gas, provided the Fe is not highly ionized. There is also evidence for an absorbed power-law component in both spectra, which we attribute to a background ultraluminous X-ray source.

Key words: circumstellar matter – hydrodynamics – supernovae: general – supernovae: individual (SN 2010jl) – X-rays: general

Online-only material: color figures

1. INTRODUCTION

Supernova (SN) 2010jl was discovered on 2010 November 3.5 (UT) at a magnitude of 13.5 (Newton & Puckett 2010), and brightened to magnitude 12.9 over the next day, showing that it was discovered at an early phase. Pre-discovery observations indicate an explosion date in early 2010 October (Stoll et al. 2011). Spectra on 2010 November 5 show that it is a Type IIn event (Benetti et al. 2010). The apparent magnitude is the brightest for a Type IIn SN since SN 1998S. SN 2010jl is associated with the galaxy UGC 5189A at a distance of 50 Mpc ($z = 0.011$), implying that SN 2010jl reached $M_V \sim -20$ (Stoll et al. 2011) and placing it among the more luminous Type IIn events (Kiewe et al. 2012). *Hubble Space Telescope* (*HST*) images of the site of the SN taken a decade before the SN indicate that, unless there is a chance coincidence of a bright star with the SN site, the progenitor star had an initial mass $\gtrsim 30\ M_\odot$ (Smith et al. 2011). Optical spectra give evidence for a dense circumstellar medium (CSM) expanding around the progenitor star with speeds of 40–120 km s^{-1} (Smith et al. 2011). Stoll et al. (2011) found that the host galaxy is of low metallicity, supporting the emerging trend that luminous SNe occur in low-metallicity environments. They determine the metallicity Z of the SN region to be $\lesssim 0.3\ Z_\odot$.

Spitzer observations showed a significant infrared (IR) excess in SN 2010jl, indicating either new dust formation or the heating of circumstellar dust in an IR echo (Andrews et al. 2011). Andrews et al. (2011) attributed the IR excess to pre-existing dust and inferred a massive CSM around SN 2010jl. Smith et al. (2012) found signatures of new dust formation in the post-shock shell of SN 2010jl from their multi-epoch spectra. While a significant IR excess is present, the SN does not show large reddening, indicating that the dust does not have a spherically symmetric distribution about the SN (Andrews et al. 2011). The *Swift* onboard X-ray Telescope (XRT) detected X-rays from SN 2010jl on 2010 November 5.0–5.8 (Immler et al. 2010). Assuming a temperature of 10 keV and a Galactic absorption column of $N_H = 3.0 \times 10^{20}$ cm^{-2}, Immler et al. (2010) obtained an unabsorbed X-ray luminosity of $(3.6 \pm 0.5) \times 10^{40}$ erg s^{-1} in the 0.2–10 keV band.

After the detection of SN 2010jl with the *Swift*-XRT, we triggered *Chandra* observations of the SN at two epochs, in 2010 December and 2011 October, and we present the results here (Section 2). We discuss the significant changes in the two *Chandra* observations taken 10 months apart in Section 3.

2. OBSERVATIONS AND ANALYSIS

2.1. Observations

The *Swift* detection of SN 2010jl allowed us to trigger our approved *Chandra* Cycle 11 program in 2010 December. We again observed SN 2010jl in 2011 October under Cycle 13 of *Chandra*. The first observation (Figure 1) took place under proposal 11500430 starting 2010 December 7 at 04:22:53 hr (UT) for an exposure of 19.05 ks and then on 2010 December 8 at 00:50:20 hr (UT) for a 21.05 ks exposure. The observations were taken with ACIS-S without grating in a VFAINT mode. A total of 39.58 ks exposure time was used in the data analysis and 468 counts were obtained with a count rate of $(1.13 \pm 0.05) \times 10^{-2}$ counts s^{-1}. The second set of observations (Figure 2) took place under our proposal 13500593 starting on 2011 October 17 at 20:25:09 hr (UT) for an exposure of 41.04 ks. The observations were again taken with ACIS-S in the VFAINT mode with grating NONE. From a total of 40.51 ks usable

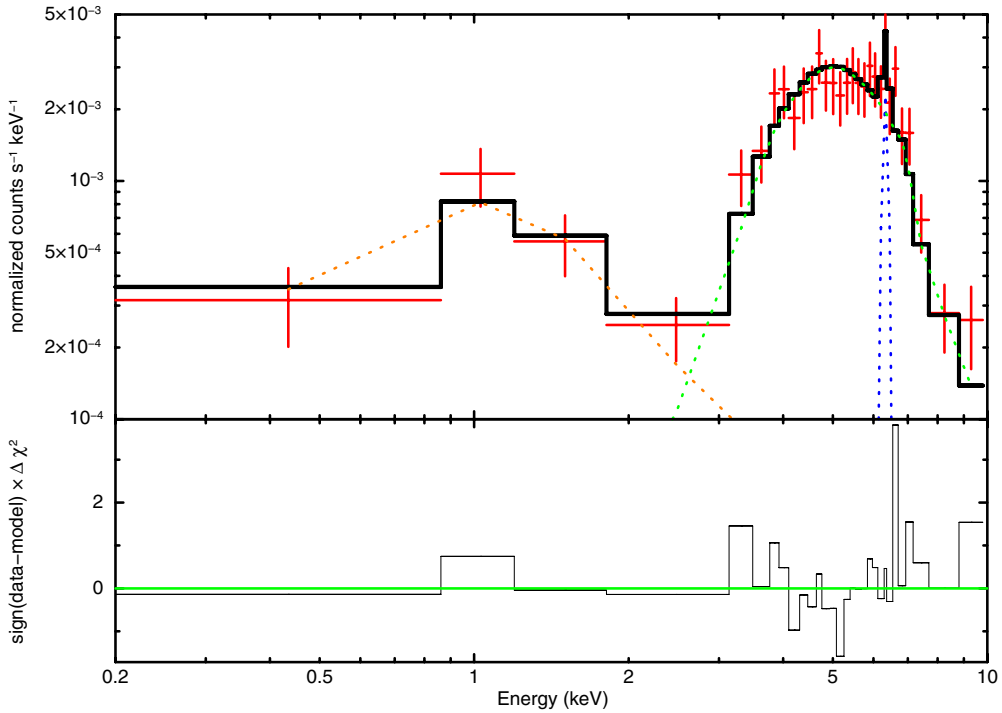

Figure 1. Best-fit *Chandra* spectrum of SN 2010jl taken in 2010 December. The spectrum is best fit with a high-T, high-$N_{\rm H}$ thermal component, a Gaussian at 6.4 keV, and a power law with photon index $\Gamma = 1.76$.

(A color version of this figure is available in the online journal.)

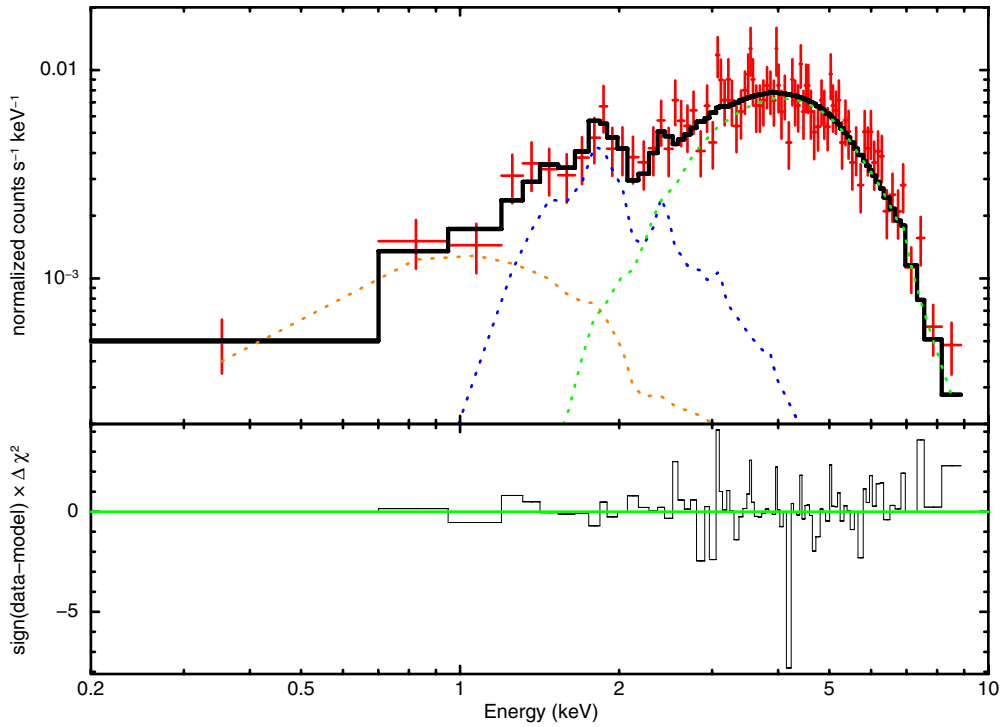

Figure 2. Best-fit *Chandra* spectrum of SN 2010jl taken in 2011 October. The plot is for the model when the column densities of both temperature components (green dashed line and the blue dashed line) are allowed to vary independently in the fit.

(A color version of this figure is available in the online journal.)

exposure time, we obtained 1342 total counts, i.e., a count rate of $(3.29 \pm 0.09) \times 10^{-2}$ counts s^{-1}. We extracted the spectra using CIAO software[6] and used HEAsoft[7] to carry out the spectral analysis.

[6] http://asc.harvard.edu/ciao/

[7] http://heasarc.gsfc.nasa.gov/docs/software/lheasoft/

2.2. Spectral Analysis

As can be seen in Figures 1 and 2, the normalized count rate is higher in the 2011 October spectra. This does not necessarily indicate higher intrinsic emission from the SN at the later time, because the count rates are absorbed count rates and the unabsorbed emission depends on the intervening column

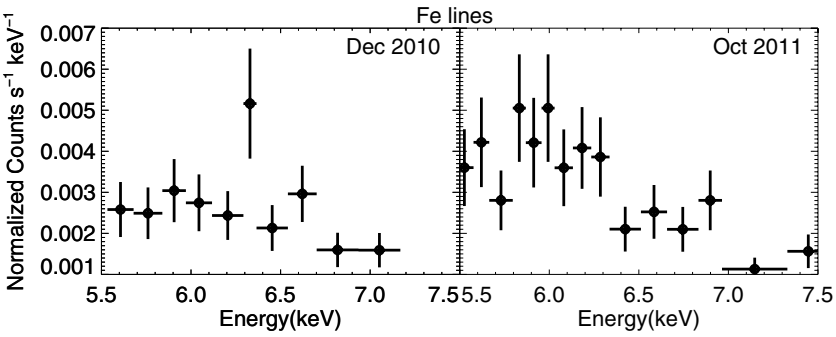

Figure 3. Comparison of the 2010 December and 2011 October spectra around the Fe 6.4 keV line energy. The line is clearly visible at the early time, but not at the later time.

Table 1
Spectral Model Fits to the SN 2010jl Spectra

Spectrum	Model	χ^2/ν	$N_{\rm H}$	Parameter	Abs. Flux	Unabs. Flux
2010 Dec	**Mekal**	0.84(23)	$9.70^{+1.60}_{-1.61} \times 10^{23}$	$kT = 79.9^{+\cdots}_{-68.03}$	6.55×10^{-13}	2.44×10^{-12}
	+ Gaussian	···	···	$E = 6.32^{+0.06}_{-0.06}$	2.43×10^{-14}	4.25×10^{-14}
	+ PowerLaw	···	3.0×10^{20} (fixed)	$\Gamma = 1.68^{+0.66}_{-0.72}$	1.21×10^{-14}	1.29×10^{-14}
	Mekal	0.87(24)	$10.59^{+1.77}_{-1.28} \times 10^{23}$	$kT = 8.0$ (fixed)	5.57×10^{-13}	3.23×10^{-12}
	+ Gaussian	···	···	$E = 6.32^{+0.06}_{-0.06}$	3.02×10^{-14}	5.56×10^{-14}
	+ PowerLaw	···	3.0×10^{20} (fixed)	$\Gamma = 1.63^{+0.70}_{-0.64}$	1.18×10^{-14}	1.24×10^{-14}
2011 Oct	**Mekal**	0.92(75)	$2.67^{+3.47}_{-0.48} \times 10^{23}$	$kT = 79.9^{+\cdots}_{-68.55}$	1.04×10^{-12}	2.13×10^{-12}
	+ Mekal	···	$8.38^{+0.52}_{-0.43} \times 10^{22}$	$kT = 1.05^{+0.95}_{-0.44}$	3.76×10^{-14}	4.94×10^{-13}
	+ PowerLaw	···	3.0×10^{20} (fixed)	$\Gamma = 1.54^{+0.73}_{-0.71}$	2.37×10^{-14}	2.42×10^{-14}
	Mekal	0.99(78)	$3.51^{+2.52}_{-1.14} \times 10^{23}$	$kT = 12$ (fixed)	9.49×10^{-13}	2.62×10^{-12}
	+ Mekal	···	$9.06^{+3.95}_{-2.42} \times 10^{22}$	$kT = 1.15^{+1.41}_{-0.53}$	5.34×10^{-14}	5.87×10^{-13}
	+ PowerLaw	···	3.0×10^{20} (fixed)	$\Gamma = 1.76^{+0.81}_{-0.84}$	1.97×10^{-14}	2.15×10^{-14}

Notes. Here, $N_{\rm H}$ is in cm^{-2}, E is in keV, and the fluxes are in erg cm^{-2} s^{-1}. The fluxes are given in the 0.2–10.0 keV energy range. The absorbed and unabsorbed fluxes are for that particular component in the model. The errors in the fluxes are 20%–30%.

density, which may change. In the 5.5–7.5 keV range, the fluorescent 6.4 keV Fe line is present in the first spectrum but not the second (Figure 3). Here we carry out a detailed spectral analysis of both spectra and determine the significance of various emission components along with the Fe 6.4 keV line.

2.2.1. 2010 December Spectrum

For the 2010 December spectrum, we first fit the high-temperature component in the 2–10 keV energy range, where most of the emission in the *Chandra* energy band lies. We fit the spectrum in this range with an absorbed Mekal model (Mewe et al. 1985; Liedahl et al. 1995) with metallicity $Z = 0.3\,Z_{\odot}$ (Stoll et al. 2011). The preferred Mekal temperature always hits the upper bound of the temperature allowed in the Mekal model, i.e., 79.9 keV. The column density is also very high, with $N_{\rm H} \approx 10^{24}$ cm^{-2}. Since the temperature in the best-fit models seems high, we checked for the possibility of a non-thermal X-ray emission and fit a power-law model. The column density in this fit is consistent with that of the Mekal model; however, the photon index is too small to be physically plausible ($\Gamma = 0.33$), and we disfavor the non-thermal model.

When we plot the confidence contours of $N_{\rm H}$ versus kT, the column density in our fits is well constrained, but the upper bound of the temperature is not constrained (Figure 4). We established a lower bound on the temperature by assuming a value and finding the goodness of fit; $T = 8$ keV gives a good fit with acceptable χ^2 value, but not lower values. Thus, 8 keV is a lower limit on the temperature of the main X-ray emission component of the SN. For the lower temperature component in the 0.2–2 keV range, we fix the absorption column to the Galactic value of 3.0×10^{20} cm^{-2} since the absorption column for this component is very poorly constrained. This component is best fit with a temperature of ∼2 keV or a power law with $\Gamma = 1.76$.

Figure 1 shows the best fit to the *Chandra* spectrum taken between 2010 December 07.18 UT and 08.03 UT, and the best fits are tabulated in Table 1. Our complete model is the Absorption×Powerlaw + Absorption×(Mekal + Gaussian). 97.9% of the total unabsorbed flux in the *Chandra* band is carried by the high-temperature component. The Fe 6.4 keV line carries 1.7% of the total flux while the low-$N_{\rm H}$ component only has 0.4% of the total flux. The rest energy of the Fe line is 6.39 ± 0.06 keV, which is consistent with the Kα line. The equivalent width of the line is $\mathrm{EW_{Fe}} = 0.2 \pm 0.1$ keV.

2.2.2. 2011 October Spectrum

The *Chandra* spectrum taken between 2011 October 17.85–18.33 UT is different from the first epoch spectrum. We first fit the high-temperature component between 2 and 10 keV. The temperature in this case also reaches the Mekal model upper limit of 79.9 keV. To consider the possibility of non-thermal emission, we fit a power law to the spectrum. However, the power-law fit to this component yields a photon index of $\Gamma = 0.45$, which is implausible.

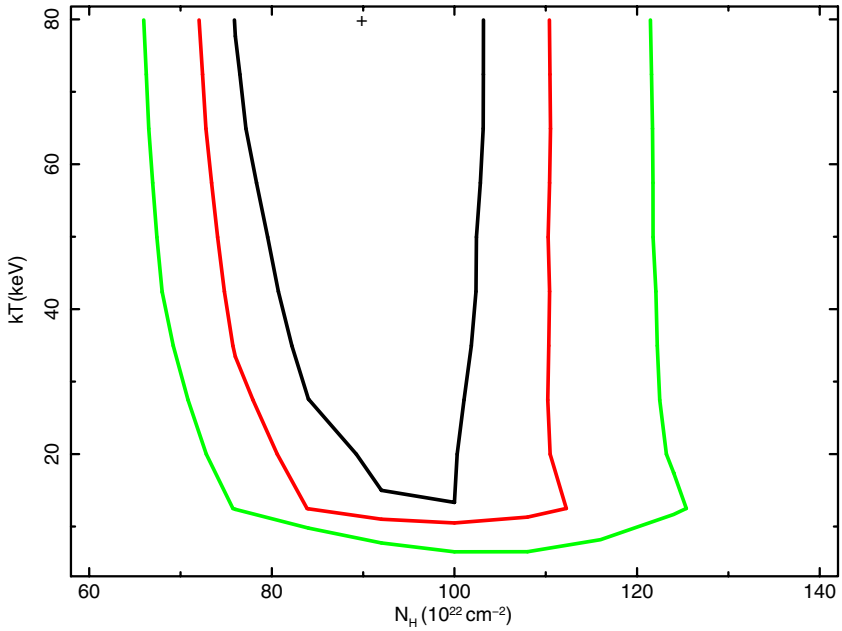

Figure 4. Plot shows 68% (black), 90% (red), and 99% (green) confidence contours for the $N_{\rm H}$ vs. kT confidence contours plot for the 2010 December spectrum. The column density is well constrained while the temperature is unconstrained on the high side.

(A color version of this figure is available in the online journal.)

In this spectrum, the column density has decreased by a factor of three; the best-fit column density for $Z = 0.3\,Z_{\odot}$ is $\sim 3 \times 10^{23}$ cm^{-2}. The Fe 6.4 keV line is not present, but the low-temperature component is there. Because of few data points and a large uncertainty in the column density in this component, we again fix the column density to the Galactic value. When we fit the low-temperature component with a thermal plasma or a power-law model, it fits with a temperature of $\sim$1–2 keV or a power law of $\sim$1.7. However, another component is still required by the data. When we try to fit this component using the same column density as that of the main emission component, we find $T = 0.11$ keV and a very high unabsorbed luminosity $\sim 10^{45}$ erg s^{-1}, which is implausible. Thus, we try to fit this component with an independently varying column density. The column density associated with this component is around 1/4 that of the high-$N_{\rm H}$ component column density. This gives a reasonable and physically plausible component and indicates that the flux is this component is 15%–20% of the total emission. Thus, in this spectrum, we have three components: a high-$N_{\rm H}$ high-T component, a high-$N_{\rm H}$ low-T component, and a low-$N_{\rm H}$ component.

Although the preferred temperature again reaches the upper bound allowed by the Mekal model, the error determination shows that there is no upper bound and the lower bound to the temperature is 12 keV. Our final model thus is Absorption×Power law + Absorption×Mekal+Absorption×Mekal. Figure 2 shows the best fit to the *Chandra* 2011 October spectrum. Table 1 lists the models and best-fit parameters. In this case, 81.1% of the unabsorbed flux is carried by the high column density component, 18.2% by the lower-$N_{\rm H}$ component, and 0.7% is carried by the power-law component.

3. RESULTS AND INTERPRETATION

Here we highlight the main differences between the 2010 December and 2011 October spectra and discuss the best-fit models and their implications. The lower limits on the temperature for the two spectra are 8 keV and 12 keV, respectively, showing that a hot component is present. The column densities of the main X-ray emission component (high-$N_{\rm H}$ component) are high at both epochs. The column densities at the first and second epochs are $\sim 10^{24}$ cm^{-2} and 3×10^{23} cm^{-2} (for a metallicity of $Z \approx 0.3\,Z_{\odot}$), respectively. These are 3000 times and 1000 times higher than the Galactic column density (3×10^{20} cm^{-2}). The high value and variability of $N_{\rm H}$ point to an origin in the CSM. The excess column density to the X-ray emission is not accompanied by high extinction to the SN, showing that the column is probably due to mass loss near the forward shock wave where any dust has been evaporated. This is the first time that external circumstellar X-ray absorption has been clearly observed in an SN.

Assuming 2010 October 10 as the date of explosion (Andrews et al. 2011; Patat et al. 2011), the epochs of the two *Chandra* observations are 59 and 373 days, respectively. The 0.2–10 keV absorbed flux at the second epoch (1.1×10^{-12} erg cm^{-2} s^{-1}) is higher than that at the first epoch (6.5×10^{-13} erg cm^{-2} s^{-1}), but this is due to the lower absorption column density at the second epoch. The actual unabsorbed emission from the SN is constant within 20%–30%. At the two epochs, the unabsorbed luminosity in the 0.2–10 keV band is $\sim 7 \times 10^{41}$ erg s^{-1}, placing SN 2010jl among the most luminous X-ray SNe yet observed. Table 1 of Immler (2007) shows that the only other SNe with comparable luminosities are Type IIn events or gamma-ray burst associated SNe at early times. The luminosity of $3.6 \pm 0.5 \times 10^{40}$ erg s^{-1} found by *Swift* on 2010 November 5 (Immler et al. 2010) is revised to a value close to our *Chandra* result if $N_{\rm H} \sim 10^{24}$ cm^{-2} is assumed. In the thermal interpretation, the shock velocity can be deduced as $v_{\rm sh} = [16\,kT/(3\mu)]^{1/2} = 7700(kT/80\,{\rm keV})^{1/2}$ km s^{-1}, where k is Boltzmann's constant and μ is the mean particle weight. A lower limit of 10 keV for the temperature puts a lower limit of the 2700 km s^{-1} on the shock speed.

In comparing the observed luminosity to a thermal emission model to find the physical parameters, we note that our measurements give the spectral luminosity, not the total luminosity. We use Equation (3.11) of Fransson et al. (1996) for the luminosity,

adjusting to an observed photon energy of ∼10 keV rather than 100 keV; the Gaunt factor is increased to 2–3. For the pre-shock column density, we use Equation (4.1) of Fransson et al. (1996). These expressions allow for a variation of the pre-shock density $\propto r^{-s}$, where s is a constant. The value $s = 2$ corresponds to a steady wind and is commonly used, but implies stronger evolution than we observe in SN 2010jl. If the CSM around SN 2010jl is due to some pre-SN eruptive event, deviation from $s = 2$ is plausible. Another parameter is m, determined by the expansion of the SN shock $R \propto t^m$. For the plausible value $m = 0.8$, we find that $s = 1.6$ gives a reasonable representation of the luminosity and $N_{\rm H}$ evolution. The implied value of the mass loss rate $\dot{M}$, normalized to $R = 10^{15}$ cm, is $\dot{M}_{-3}/v_{w2} \approx 8 v_4^{0.6}$, where $\dot{M}_{-3} = \dot{M}/(10^{-3}\, M_\odot\, {\rm yr}^{-1})$, v_{w2} is the pre-shock wind velocity in units of 100 km s^{-1}, and v_4 is the shock velocity in units of 10^4 km s^{-1} at the first epoch.

The high temperature implies that we are observing the forward shock region. The physical conditions are such that the forward shock front is close to the cooling regime (Chevalier & Irwin 2012). In this case, the luminosity of the forward shock is expected to dominate that from the reverse shock and the reverse shock emission may be absorbed by a cooled shell, which explains the lack of observational evidence for reverse shock emission.

In modeling the X-ray absorption in SN 2010jl we have assumed that the absorbing gas is not fully ionized. If the circumstellar gas is photoionized by the X-ray emission, the absorption is reduced (e.g., Fransson 1982). Taking an X-ray luminosity of 10^{42} erg s^{-1} and $\dot{M}_{-3}/v_{w2} \approx 8$ (at $r = 10^{15}$ cm), the ionization parameter is $\zeta = L/nr^2 \approx 200$; a similar value is obtained taking $nr \sim N_{\rm H} \sim 10^{24}$ cm^{-2} and $r = 6 \times 10^{15}$ cm for the early epoch. This is in a regime where the CNO elements may be completely ionized, but Fe is not (Hatchett et al. 1976). The CNO elements absorb radiation at ∼1 keV, so there is the possibility of getting enhanced emission around that energy, as is observed in SN 2010jl. We investigated this possibility by running various cases with the CLOUDY photoionization code (Ferland et al. 1998). It is possible to obtain cases in which there is a peak at ∼1 keV, but they had too little absorption in the 1.5–3 keV range. We thus favor a background source origin for the 1 keV emission, especially because the emission remains fairly constant over the two epochs.

The value of $N_{\rm H}$ in 2010 December implies that $\tau_{\rm es} \approx 1$, where $\tau_{\rm es}$ is the electron scattering optical depth through the pre-shock wind. The Hα line at that time showed roughly symmetric broad wings (Smith et al. 2012) that are probably best explained by electron scattering in the slow moving wind. Chugai (2001) estimated that the broad features observed in SN 1998S require $\tau_{\rm es} \approx$ (3–4). The required optical depth may be several times that observed along the line of sight to the X-ray emission, which could be the result of asymmetry. Andrews et al. (2011) found that the column density of dust needed for observed infrared emission is larger than that on the line of sight to the SN, although this is at larger radii.

The 2010 December spectrum shows a 6.4 keV feature (Figure 3), which is identified with the narrow Kα iron line. Since the 6.4 keV Fe line arises from neutral or low ionized iron (Fe I to Fe XI), it supports our finding that the radiation field is not able to completely ionize the circumstellar gas. A simple estimate of the expected equivalent width of the Fe line (EW$_{\rm Fe}$) can be obtained from Equation (5) of Kallman et al. (2004): EW$_{\rm Fe} = 0.3\,(Z/Z_\odot) N_{24}$ keV, where N_{24} is the circumstellar column density in units of 10^{24} cm^{-1} and the line production is due to a central X-ray source in a spherical shell. The expression assumes a flux spectrum $F_E \propto E^{-1}$; $F_E \propto E^{-0.4}$, which is more appropriate to the hot thermal spectrum here, increases EW$_{\rm Fe}$ by 1.2. The prediction for the metallicity in our case in the early spectrum is EW$_{\rm Fe} = 0.1$ keV, and the observed value is 0.2 keV. In view of the uncertainties in the model and the observations, we consider the agreement to be adequate. At the second epoch, $N_{\rm H}$ is smaller by a factor of three, so the strength of the Fe line should be correspondingly smaller; this is consistent with the nondetection of the line. The problem with this picture is that it assumes Fe is in the low ionization stages that produce the Kα line; this requires an ionization parameter $\zeta \lesssim 5$ (Kallman et al. 2004), which is below the inferred value. One possibility is that the circumstellar gas is clumped, with a density $\gtrsim$40 times the average; another is that the K line emission is from dense gas that is not along the line of sight.

A thermal fit to the low-temperature component implies an absorbing column density of $(1.37 \pm 8.44) \times 10^{20}$ cm^{-2}, much less than the column to the hot component and consistent with the Galactic column density within the errors. This rules out the possibility that the cooler X-rays come from slow cloud shocks in the clumpy CSM or from the reverse shocks. The component is also present in the second epoch. It could arise from a pre-SN mass loss event or from an unrelated source in the direction of the SN. The components are best fit with either a thermal component ($T \sim$ 1–2 keV) or a power law with $\Gamma = 1.6$–1.7. The luminosities of this component in the 2010 December and 2011 October spectra are 3.5×10^{39} erg s^{-1} and 5×10^{39} erg s^{-1}, respectively. The luminosity range and the power-law index are compatible with a background ultraluminous X-ray source (ULX), which can typically be described by an absorbed power-law spectrum (Swartz et al. 2004). Since the error in the flux determination is between 20%–30%, a factor of 1.4 change in the luminosity at the two epochs is consistent with a constant flux. Thus we attribute this component to a background source, most likely a ULX, which is associated with the blue excess emission region seen in the pre-SN *HST* images (Smith et al. 2011). We examined the HEASARC archives for useful limits on such a source, but did not find any.

The 2010 December spectrum has only one temperature component associated with the high column density. However, in the 2011 October spectrum, there are two temperature components associated with a high column density, one with temperature $\gtrsim$10 keV and another with temperature 1.1 keV. The lower temperature component fits with 1/4 the column density of the high-temperature component. The fact that the component is absent at the first epoch suggests that it is related to the SN emission. We examined the possibility that the emission is the result of reduced absorption due to photoionization of the absorbing material, in particular, that lighter atoms are ionized but heavier atoms are not. However, we were not able to reproduce the observed emission and the source of this emission remains uncertain.

SN 2010jl is a special Type IIn SN because we have been able to catch it in X-rays early on with as sensitive an instrument as *Chandra* and trace the early X-ray evolution. We observe dramatic changes over two epochs separated by 10 months. For the first time we see clear evidence of external CSM absorption in an SN. We also find that the CSM is not fully photoionized by the SN emission, the SN is very luminous in X-rays, and the temperature of the emitting gas is $\gtrsim$10 keV.

We are grateful to the referee for useful comments. Support for this work was provided by NASA through Chandra Awards GO0-211080X and GO2-13082X issued by the Chandra X-ray Observatory Center, which is operated by the Smithsonian Astrophysical Observatory for and on behalf of NASA under contract NAS8-03060.

Facility: CXO

REFERENCES

Andrews, J. E., Clayton, G. C., Wesson, R., et al. 2011, AJ, 142, 45
Benetti, S., Bufano, F., Vinko, J., et al. 2010, CBET, 2536, 1
Chevalier, R. A., & Irwin, C. M. 2012, ApJ, 747, L17
Chugai, N. N. 2001, MNRAS, 326, 1448
Ferland, G. J., Korista, K. T., Verner, D. A., et al. 1998, PASP, 110, 761
Fransson, C. 1982, A&A, 111, 140
Fransson, C., Lundqvist, P., & Chevalier, R. A. 1996, ApJ, 461, 993
Hatchett, S., Buff, J., & McCray, R. 1976, ApJ, 206, 847
Immler, S. 2007, in Supernova 1987A: 20 Years After, ed. S. Immler, K. Weiler, & R. McCray (Melville, NY: AIP), 246
Immler, S., Milne, P., & Pooley, D. 2010, ATel, 3012, 1
Kallman, T. R., Palmeri, P., Bautista, M. A., Mendoza, C., & Krolik, J. H. 2004, ApJS, 155, 675
Kiewe, M., Gal-Yam, A., Arcavi, I., et al. 2012, ApJ, 744, 10
Liedahl, D. A., Osterheld, A. L., & Goldstein, W. H. 1995, ApJ, 438, L115
Mewe, R., Gronenschild, E. H. B. M., & van den Oord, G. H. J. 1985, A&AS, 62, 197
Newton, J., & Puckett, T. 2010, CBET, 2532, 1
Patat, F., Taubenberger, S., Benetti, S., Pastorello, A., & Harutyunyan, A. 2011, A&A, 527, L6
Smith, N., Li, W., Miller, A. A., et al. 2011, ApJ, 732, 63
Smith, N., Silverman, J. M., Filippenko, A. V., et al. 2012, AJ, 143, 17
Stoll, R., Prieto, J. L., Stanek, K. Z., et al. 2011, ApJ, 730, 34
Swartz, D. A., Ghosh, K. K., Tennant, A. F., & Wu, K. 2004, ApJS, 154, 519